Gaussian noise and quantum-optical communication

Michael J. W. Hall
Department of Theoretical Physics, Australian National University, Canberra, Australian Capital Territory 0200, Australia
(Received 7 June 1993; revised manuscript received 11 January 1994)

The description of Gaussian noise for single-mode quantum fields is briefly reviewed and applied to calculate the maximal information properties of three quantum communication channels degraded by Gaussian noise. These channels are based on (i) heterodyne detection of coherent states, (ii) homodyne detection of squeezed states, and (iii) photodetection of number states. It is found that each channel can outperform the others for a given noise level, where the optimum channel is essentially determined by the product of the average noise and signal energies.

PACS number(s): 42.50.Ar, 42.50.Dv, 89.70.+c

I. INTRODUCTION

The quantum theory of light insists on a statistical description for the properties of electromagnetic fields. However, even in the classical theory, statistics are already required to model phenomena such as thermal radiation, refractive index fluctuations, and scattering by random media [1,2]. In general, such phenomena provide unwanted noise and in optical communication theory lead to the problems of detection and estimation of optical signals in the presence of noise [3,4].

For narrow-band classical fields, the most commonly considered noise model is (additive) Gaussian noise [2,3]. The ubiquity of this model arises via the central limit theorem [2], which implies that the sum of many independent random disturbances will typically have a Gaussian distribution. Gaussian noise further provides a worst-case scenario for the information properties of classical communication channels [5] and is therefore useful in investigating the performance limits of such channels.

The analog of Gaussian noise for narrow-band quantum fields is of obvious interest as a generic noise model for quantum-optical systems and was first considered by Glauber [6] for the case of the vacuum state. Various generalizations have since been obtained to describe noise added to coherent states [7,8] (see also Sec. V.4 of [4]), squeezed coherent states [9,10], and photon number states [11,12]. Some general properties were considered in [13] and applied to obtain an upper bound for the mutual information of narrow-band quantum channels degraded by Gaussian noise.

In Sec. II of this paper, the quantum representation of Gaussian noise is derived for *arbitrary* states, in a manner which clearly demonstrates its generic nature. No appeals are made to thermal radiation, quasiprobability distributions, chaotic light, or master equations. Some basic properties of quantum Gaussian noise, necessary for the purposes of calculation, are briefly noted.

In Sec. III the channel capacities of three narrow-band quantum channels degraded by Gaussian noise are calculated. These channels are based respectively on heterodyne detection of coherent states, homodyne detection of squeezed-coherent states, and photodetection of photon-number states. Results are compared in Sec. III E and it is found that the qualitative features differentiating performance depend upon the *product* of the average signal and noise energies. In particular, the number, squeezed, and coherent-state channels become optimal in turn as this product increases. Conclusions are presented in Sec. IV.

II. GENERIC NATURE AND PROPERTIES OF GAUSSIAN NOISE

A. Gaussian noise model

The simplest approach to quantum Gaussian noise is to consider, in direct analogy with the classical case [2], a single-mode field subject to displacements $\beta_1, \beta_2, \ldots, \beta_n$ at times $t_1, t_2, \ldots, t_n$, respectively. For quantum fields, such displacements are implemented via the Glauber displacement operator

$$D(\beta)=\exp(\beta a^\dagger-\beta^* a) , \quad (1)$$

and hence, assuming free-field evolution between successive displacements, the state of the field at time $t \geq t_n$ is described by the density operator

$$\rho'=U(t)\rho U^\dagger(t) , \quad (2)$$

where ρ is the initial density operator and $U(t)$ denotes the unitary operator

$$\begin{aligned} U(t)&=e^{-iN\omega(t-t_n)}D(\beta_n)e^{-iN\omega(t_n-t_{n-1})}\cdots e^{-iN\omega(t_2-t_1)}D(\beta_1)e^{-iN\omega t_1} \\ &=e^{-iN\omega t}D(\beta_n e^{i\omega t_n})\cdots D(\beta_1 e^{i\omega t_1}) \\ &=e^{i\chi}e^{-iN\omega t}D(\beta_1 e^{i\omega t_1}+\cdots+\beta_n e^{i\omega t_n}) . \end{aligned} \quad (3)$$

[In Eq. (3), N is the photon-number operator and $e^{i\chi}$ is an unimportant phase factor.] In the equivalent Heisenberg picture the modal amplitude a' at time $t \geq t_n$ is thus related to the initial amplitude a by

$$a' = U^\dagger(t) a U(t) = e^{-i\omega t}(a + \beta_1 e^{i\omega t_1} + \cdots + \beta_n e^{i\omega t_n}) , \quad (4)$$

just as for the classical case [2].

It is seen from Eq. (3) that the displacements correspond to adding linear terms to the free-field Hamiltonian, viz.,

$$H = \hbar\omega(N + \tfrac{1}{2}) + i\hbar \sum_{j=1}^{n} \delta(t - t_j)[\beta_j a^\dagger - \beta_j^* a] . \quad (5)$$

Such terms can model either the interaction of the mode with classical field amplitudes β_j or radiation into the mode from a classical current [6]. Note that more generally the displacements may act over nonvanishing time periods rather than as δ-function spikes as in (5), still leading to an overall displacement of the field of the form (3) [6].

Now suppose that the interaction process is of a random nature, so that the quantities $\beta_1 \exp(i\omega t_1), \ldots, \beta_n \exp(i\omega t_n)$ are random variables. The statistics of their sum β is then modeled by some classical probability distribution $p(\beta)$, and the state of the field at time $t \geq t_n$ follows from (2) and (3) as $e^{-iN\omega t} D(\beta)\rho D^\dagger(\beta) e^{iN\omega t}$ with probability $p(\beta)$. An *ensemble* of such fields is therefore described by the averaged density operator [14]

$$\rho_t = e^{-iN\omega t}\left[\int d^2\beta\, p(\beta) D(\beta)\rho D^\dagger(\beta) \right] e^{iN\omega t} . \quad (6)$$

Since the predictions of quantum mechanics deal only with ensembles, the effect of random displacements on the statistics of the field is completely described by (6). The randomness leads to a mixed-state description of the field in general, even when the initial state is pure [cf. Eq. (9.24) of [6] for the case of a (multimode) field initially in a vacuum state].

The distribution $p(\beta)$ in (6) is in general determined by the environment of the field. However, the central limit theorem states that under quite general conditions the sum of a large number of independent amplitudes tends to be *Gaussian* distributed [2]. In particular, if the quantities $\beta_1 \exp(i\omega t_1), \ldots, \beta_n \exp(i\omega t_n)$ are stochastically independent, with zero means and random phases, and if n is sufficiently large, then the statistics of their sum β can typically be modeled by a distribution of the form

$$p(\beta) \equiv p_\gamma(\beta) = (\pi n_\gamma)^{-1} \exp(-|\beta|^2/n_\gamma) , \quad (7)$$

where n_γ is a variance parameter. Environments modeled by Eqs. (6) and (7) may be called *Gaussian* noise sources and include thermal radiation, gas discharges, Cerenkov radiation, and other noncoherent macroscopic light sources [6,7]. A further example is the zero-gain linear amplifier (see Sec. II B).

Gaussian noise, as defined by (6) and (7), has been commonly referred to in the literature as "thermal noise" [4,7–10,12,15]. There are, however, a number of sound reasons for avoiding the latter label. First, as mentioned above, Gaussian noise provides a noise model applicable to many different scenarios, so that the label "thermal" is unduly restrictive. Second, it is important to distinguish Gaussian noise from entirely different types of noise that have also been labeled "thermal" in the literature [16–18]. Third, an early motivation for labeling Gaussian noise as thermal turns out to be misleading. Glauber suggested in [6] that the "superposition" of two fields be represented by the convolution of P representations, leading Lachs [7] and Lee [15] to define thermal noise as arising from superposition with a *thermal* state. While such thermal noise is equivalent to Gaussian noise [p_γ in Eq. (7) is the P representation of $\rho_{\rm th}$ [6]], the basis of this superposition approach to Gaussian noise is conceptually flawed: the convolution of two P representations does not in general yield the P representation of any state (consider the case of two number states). Similar remarks apply to the approach of Loudon and Shepherd [11], which equivalently seeks to represent the superposition of two fields by the multiplication of normally ordered characteristic functions.

Finally, it may be remarked here that Gaussian noise as defined by (6) and (7) could more exactly be referred to as Gaussian *displacement* noise. This would serve, for example, to distinguish (6) from the Gaussian *phase* noise process,

$$F(\rho) = \int_{-\infty}^{\infty} d\phi\, p(\phi) \exp(iN\phi)\rho \exp(-iN\phi) , \quad (8)$$

where $p(\phi)$ is a Gaussian distribution on the real line.

B. Properties

No systematic exposition of Gaussian noise for quantum fields appears to have been given in the literature. Here several basic properties required for calculations in Sec. III are noted. Attention is focused on the mapping $\rho \to \Gamma(\rho)$ defined by

$$\Gamma(\rho) = \int d^2\beta\, p_\gamma(\beta) D(\beta)\rho D^\dagger(\beta) , \quad (9)$$

with $p_\gamma(\beta)$ as in (7), since (i) the exponential factors in (6) represent free-field evolution, which is well understood, and (ii) these exponential factors can be removed by transforming to the interaction picture [Eq. (19a) below]. It is convenient to adopt a notation whereby if Q denotes some quantity calculated for state ρ, then Q_Γ denotes that quantity calculated for the state $\Gamma(\rho)$.

First, for the normally ordered moment

$$M^{k,l} = \mathrm{tr}[(a^\dagger)^k a^l \rho] \quad (10)$$

of state ρ, it follows as per Eq. (10) of [13] that

$$M_\Gamma^{k,l} = \sum_{r=0}^{\min(k,l)} \binom{k}{r} \binom{l}{r} r!\, n_\gamma^r M^{k-r,l-r} . \quad (11)$$

Choosing $k = l = 1$ yields

$$\langle N \rangle_\Gamma = \langle N \rangle + n_\gamma , \quad (12)$$

and thus the variance parameter n_γ may be interpreted as the average noise energy added to the field. Evaluating the quadrature and photon-number variances via (11) leads to the result that just *half a photon of Gaussian noise is sufficient to destroy all quadrature and intensity squeezing* for any state.

Second, let χ denote the normally ordered characteristic function for state ρ [19,20]. From (7) and (9) one has

$$\begin{aligned}\chi_\Gamma(\xi)&=\mathrm{tr}[e^{i\xi^* a^\dagger}e^{i\xi a}\Gamma(\rho)]\\&=\int d^2\alpha\, p_\gamma(\alpha)\mathrm{tr}[e^{i\xi^*(a^\dagger-\alpha^*)}e^{i\xi(a-\alpha)}\rho]\\&=\exp(-n_\gamma|\xi|^2)\chi(\xi)\ .\end{aligned}\tag{13}$$

[It is worthwhile noting that the relationships between the normally ordered, antinormally ordered, and Wigner characteristic functions and their corresponding moments [19] imply that Eqs. (11) and (13) in fact hold for all three orderings.] Equation (13) may be recognized as the characteristic function of a state subject to linear amplification for time t (identifying n_γ with σNt, where σ is a rate constant and N is the total number of amplifier atoms [21–23]), in the case of zero gain. Thus the corresponding master equation [21–23] provides a dynamical model for Gaussian noise. Note that this master equation may be solved to give an explicit perturbation expansion

$$\Gamma(\rho)=(1-z)\sum_m \frac{z^m}{m!}\sum_{r,s=0}^{m}\begin{bmatrix} m\\ r\end{bmatrix}\begin{bmatrix} m\\ s\end{bmatrix}(-1)^{r+s}(a^\dagger)^{m-r}a^s\rho(a^\dagger)^r a^{m-s}\tag{14}$$

for Gaussian noise [24], with $z=n_\gamma/(n_\gamma+1)$, which is useful for numerical calculations when n_γ is small.

Third, a formula for the number-state matrix element $\langle m|\Gamma(\rho)|n\rangle$ in terms of the matrix elements of ρ can be derived following Vourdas [12], yielding

$$\langle n+j|\Gamma(\rho)|n\rangle=\sum_k R_{nk}^{(j)}(n_\gamma)\langle k+j|\rho|k\rangle\ ,\tag{15a}$$

where $R^{(j)}$ is the symmetric matrix function with coefficients

$$R_{nk}^{(j)}(n_\gamma)=R_{kn}^{(j)}(n_\gamma)=\frac{n_\gamma^{n+k}}{(n_\gamma+1)^{n+k+1}}\sum_{r=0}^{\min(n,k)} n_\gamma^{-2r}\left[\begin{bmatrix} n\\ r\end{bmatrix}\begin{bmatrix} k\\ r\end{bmatrix}\begin{bmatrix} n+j\\ r+j\end{bmatrix}\begin{bmatrix} k+j\\ r+j\end{bmatrix}\right]^{1/2}\ .\tag{15b}$$

Choosing $j=0$ in (15a) yields the number-state distribution of $\Gamma(\rho)$ in terms of the number-state distribution of ρ, and for this case one has

$$R_{nk}^{(0)}(v)=\frac{(1-v)^n v^{k-n}}{(1+v)^{k+1}}P_n^{(k-n,0)}\left[\frac{1+v^2}{1-v^2}\right]\tag{16}$$

for $n\le k$, where $P_n^{(\alpha,\beta)}(x)$ is a Jacobi polynomial [25]. More generally, (15a) and the property

$$\Gamma_v\circ\Gamma_w=\Gamma_{v+w}\tag{17}$$

derivable from (9) (where Γ_v denotes Gaussian noise of variance v) imply that

$$R^{(j)}(v)=\exp(vA^{(j)})\ ,\tag{18a}$$

where $A^{(j)}$ is a constant matrix. The coefficients of $A^{(j)}$ may be calculated from (15b) and (18a) as

$$A_{nk}^{(j)}=\frac{d}{dv}R_{nk}^{(j)}(v)\Big|_{v=0}=-(2n+1)\delta_{nk}+[n(n+j)]^{1/2}\delta_{n,k+1}+[(n+1)(n+j+1)]^{1/2}\delta_{n+1,k}\ .\tag{18b}$$

Equations (15), (16), and (18) will be used in Sec. III D and the Appendix to calculate information properties of number-state channels degraded by Gaussian noise.

Finally, three useful invariance properties of Gaussian noise will be noted here, which follow from (9) and properties of the Glauber displacement operator [6,19]:

$$\Gamma(e^{iN\theta}\rho e^{-iN\theta})=e^{iN\theta}\Gamma(\rho)e^{-iN\theta}\ ,\tag{19a}$$

$$\Gamma(D(\alpha)\rho D^\dagger(\alpha))=D(\alpha)\Gamma(\rho)D^\dagger(\alpha)\ ,\tag{19b}$$

$$\mathrm{tr}[A\Gamma(B)]=\mathrm{tr}[\Gamma(A)B]\ .\tag{19c}$$

The addition of Gaussian noise in the interaction representation $\tilde{\rho}_t=\exp(iN\omega t)\rho_t\exp(-iN\omega t)$ follows from (6) and (19a) simply as $\tilde{\rho}_t=\Gamma(\tilde{\rho}_0)$, emphasizing the fundamental role of the mapping Γ in describing Gaussian noise for quantum fields. Equation (19b) implies that adding noise before or after a displacement leads to the same result, and further implies simple representations for the effect of Gaussian noise on heterodyne and homodyne statistics (Sec. III). Equation (19c) proves useful for simplifying expectation values of the form $\mathrm{tr}[A\Gamma(\rho)]$ in cases where $\Gamma(A)$ may be easily evaluated.

III. APPLICATION TO NARROW-BAND COMMUNICATION

A. Notation

For a narrow-band optical channel, with center-frequency f and bandwidth $B\ll f$, a selected transverse mode is held fixed and the symbols are encoded on an orthogonal set of longitudinal modes. The narrow-band restriction allows each symbol s_j to be represented by a density operator ρ_j corresponding to a single-mode field of frequency f, and the average transmission rate is B symbols per unit time [18,26]. To enable discussion of as wide a class as possible of measurements at the receiver (including heterodyne detection in Sec. III B), it will be assumed only that the measured quantity A is represented by a *probability operator measure* [4,18,27]; i.e., by a set of positive operators $\{A_k\}$ that sum to the identity operator, and such that the probability of output value a_k for input state ρ is given by $\mathrm{tr}[A_k\rho]$.

The *mutual information* per symbol for such a channel, representing the quantity of information that may be transmitted over the channel without error, is given by [5,18]

$$I = H(A|\Sigma_j \xi_j \rho_j) - \Sigma_j \xi_j H(A|\rho_j) , \tag{20a}$$

where state ρ_j is transmitted with probability ξ_j, and

$$H(A|\rho) = -\Sigma_k \mathrm{tr}[A_k\rho] \ln \mathrm{tr}[A_k\rho] \tag{20b}$$

denotes the entropy of the output distribution for input state ρ. The logarithm base in (20b) can be chosen as any number $b>1$, with the choices $b=2$ and $b=e$ corresponding to units of "bits" and "nats," respectively.

Maximizing the mutual information subject to any channel constraints yields the *capacity* of the channel [5]. A general upper bound for the capacity of narrow-band quantum channels degraded by Gaussian noise of variance n_γ is given by [13]

$$\begin{aligned} I_{\text{quantum}}(n_s, n_\gamma) \le \ln\left[1+\frac{n_s}{n_\gamma+1}\right] &+ (n_s+n_\gamma)\ln\left[1+\frac{1}{n_s+n_\gamma}\right] \\ &- n_\gamma \ln\left[1+\frac{1}{n_\gamma}\right] , \end{aligned} \tag{21}$$

where

$$n_s = \Sigma_j \xi_j \mathrm{tr}[N\rho_j] \tag{22}$$

denotes the average photon number per signal. In the limit of large noise levels $(n_\gamma \to \infty)$, Eq. (21) becomes equivalent to the corresponding classical bound [5]

$$I_{\text{classical}}(n_s, n_\gamma) \le \ln\left[1+\frac{n_s}{n_\gamma}\right] . \tag{23}$$

The channel capacities of various narrow-band quantum-optical channels are examined in Secs. III B, III C, and III D below, and comparisons are made with (21) and (23).

B. Heterodyne detection of coherent states

It has been shown that under ideal conditions, optical heterodyne detection measures the (commuting) real and imaginary parts of the operator $a+b^\dagger$, where a and b represent the annihilation operators for the signal and image-band fields, respectively [18,28,29]. Heterodyne detection thus estimates the complex amplitude of the signal field, subject to image-band noise, and is therefore appropriate for extracting information from the well-defined complex amplitudes of coherent states.

For the case of uncorrelated signal and image-band fields, represented by density operators ρ and ρ_i respectively, the measurement statistics of ideal heterodyne detection are given by [30]

$$P(\beta) = \pi^{-1} \mathrm{tr}[D(\beta)\tilde{\rho}_i D^\dagger(\beta)\rho] . \tag{24a}$$

Here β denotes the complex eigenvalue $\beta_1 + i\beta_2$ of $a+b^\dagger$, $D(\beta)$ is the Glauber displacement operator in (1), and $\tilde{\rho}_i$ is related to the image-band state ρ_i via the (antiunitary) transformation

$$\tilde{\rho}_i = \sum_{m,n} |m\rangle\langle n|(-1)^{m+n}\langle m|\rho_i|n\rangle^* . \tag{24b}$$

For evaluation purposes the operators in (24a) and (24b) are all defined on a single Fock space with annihilation operator a. The measurement statistics in (24a) correspond to the continuous probability operator measure $\{\pi^{-1}D(\beta)\tilde{\rho}_i D^\dagger(\beta)\}$ (see Sec. III A), where β ranges over the complex plane.

Gaussian noise in the signal and image-band fields combines additively. In particular, let the signal and image-band fields each be subject to Gaussian noise, of variances v and w respectively. It follows using Eqs. (15a), (15b), (17), (19b), (19c), (24a), and (24b) that the detection statistics can be written as

$$\begin{aligned} P_{v,w}(\beta) &= \pi^{-1} \mathrm{tr}[D(\beta)\Gamma_w(\tilde{\rho}_i)D^\dagger(\beta)\Gamma_v(\rho)] \\ &= \pi^{-1} \mathrm{tr}\{\Gamma_v[D(\beta)\Gamma_w(\tilde{\rho}_i)D^\dagger(\beta)]\rho\} \\ &= \pi^{-1} \mathrm{tr}[D(\beta)\Gamma_{v+w}(\tilde{\rho}_i)D^\dagger(\beta)\rho] . \end{aligned} \tag{25a}$$

It may similarly be shown that

$$P_{v,w}(\beta) = \pi^{-1} \mathrm{tr}[D(\beta)\tilde{\rho}_i D^\dagger(\beta)\Gamma_{v+w}(\rho)] . \tag{25b}$$

From Eqs. (25) it follows that only the *sum* of the noise variances is relevant to the detection statistics.

Consider now a narrow-band communication channel based on the transmission of Glauber coherent states, which are to be resolved via ideal heterodyne detection with a vacuum-state image-band field. If the channel is subject to Gaussian noise of total variance n_γ, then the output distribution for input state ρ follows from (24) and (25b) as

$$P_\Gamma(\beta|\rho) = \pi^{-1}\langle\beta|\Gamma(\rho)|\beta\rangle , \tag{26a}$$

leading via (9) to the simple convolution relation

$$P_\Gamma = p_\gamma * P , \tag{26b}$$

where P denotes the output distribution in the absence of noise.

For the coherent input state $|\alpha\rangle\langle\alpha|$ it follows from (7), (26a), and (26b) that P_Γ is the convolution of the Gaussians p_γ and $|\langle\alpha|\beta\rangle|^2$, yielding

$$P_\Gamma(\beta|\alpha)=\pi^{-1}(n_\gamma+1)^{-1}\exp[-|\beta-\alpha|^2/(n_\gamma+1)] \ . \tag{27}$$

The capacity of the channel for a given average signal energy n_s can now be determined by maximizing the mutual information (20a) subject to the constraint

$$n_s=\int d^2\alpha\, \xi(\alpha)|\alpha|^2 \ , \tag{28}$$

where $\xi(\alpha)$ denotes the prior probability of transmitting state $|\alpha\rangle\langle\alpha|$. But Eqs. (27) and (28) are equivalent to the case of a *classical* channel with additive Gaussian noise, subject to a quadratic constraint [5], for which the optimal prior distribution is well known to be [5,18]

$$\xi(\alpha)=(\pi n_s)^{-1}\exp(-|\alpha|^2/n_s) \ . \tag{29}$$

Substitution of (27) and (29) in (20a) then yields the capacity per symbol of the channel as

$$I^{\text{coh}}(n_s,n_\gamma)=\ln\left[1+\frac{n_s}{n_\gamma+1}\right] \ . \tag{30}$$

The capacity (30) is similar to the classical capacity (23), but with a minimum "quantum noise" of one photon. A semi-classical derivation of (30) is given by Gordon in [31], which more generally predicts a minimum "quantum noise" level of ε^{-1} photons, where ε denotes the quantum efficiency of the photodetection process. For the case where no Gaussian noise is present ($n_\gamma=0$), the channel capacity is derived in [18,26].

In the limit of high noise levels ($n_\gamma\gg1$), the channel capacity (30) approaches the quantum upper bound (21), so that the coherent-state channel discussed here becomes optimal. This is related to the property that, under the addition of Gaussian noise, coherent states have the smallest increase in entropy relative to all other states [13]. However, for sufficiently low noise levels the coherent-state channel is not optimal, as will be seen below.

C. Homodyne detection of squeezed states

Ideal homodyne detection provides a sharp measurement of the quadrature-amplitude operator

$$X_\theta=\tfrac{1}{2}(ae^{i\theta}+a^\dagger e^{-i\theta}) \tag{31}$$

for some fixed value of θ, and hence is suitable for distinguishing between states characterized by well-defined quadrature-amplitude properties (e.g., quadrature-squeezed states) [18,28].

If $\{|x\rangle\}$ denotes the eigenket basis for X_θ (where x ranges over the real numbers), then the relation

$$\begin{aligned}\langle x|\Gamma(|y\rangle\langle z|)|x\rangle &=\langle x|e^{-i\lambda X_\theta}\Gamma(e^{i\lambda X_\theta}|y\rangle\langle z|e^{-i\lambda X_\theta})e^{i\lambda X_\theta}|x\rangle\\ &=e^{i\lambda(y-z)}\langle x|\Gamma(|y\rangle\langle z|)|x\rangle\end{aligned} \tag{32}$$

follows from (19b), and therefore the left-hand side of (32) vanishes unless $y=z$. But

$$\begin{aligned}\langle x|\Gamma(|y\rangle\langle y|)|x\rangle &=\int d^2\alpha\, p_\gamma(\alpha)\langle x|D(\alpha)|y\rangle\langle y|D^\dagger(\alpha)|x\rangle\\ &=\int d^2\alpha\, p_\gamma(\alpha)\langle x-\beta_1|y\rangle\langle y|x-\beta_1\rangle\\ &=(\pi n_\gamma)^{-1}\int\int d\beta_1 d\beta_2\exp[-(\beta_1^2+\beta_2^2)/n_\gamma]\delta(x-\beta_1-y)\\ &=(\pi n_\gamma)^{-1/2}\exp[-(x-y)^2/n_\gamma] \ ,\end{aligned} \tag{33}$$

where $\beta_1+i\beta_2$ denotes the decomposition of $\alpha e^{i\theta}$ into real and imaginary parts. Hence if $\hat{p}(x)=\langle x|\rho|x\rangle$ denotes the statistics of homodyne detection for state ρ, Eqs. (32) and (33) yield the simple convolution relation

$$\hat{p}_\Gamma=\hat{p}_\gamma*\hat{p} \tag{34a}$$

for the effect of Gaussian noise on the statistics of homodyne detection, where $\hat{p}_\gamma$ denotes the one-dimensional Gaussian distribution

$$\hat{p}_\gamma(x)=(\pi n_\gamma)^{-1/2}\exp(-x^2/n_\gamma) \ . \tag{34b}$$

Equation (34a) may be compared with the analogous result (26b) for the statistics of heterodyne detection.

Consider now a narrow-band channel based on the transmission of the quadrature-squeezed states

$$|y,r\rangle=D(y)S(r)|0\rangle,\quad y\in\mathbb{R},\quad r\geq0 \ , \tag{35}$$

where $S(\zeta)$ denotes the squeezing operator [32]

$$S(\zeta)=\exp[\tfrac{1}{2}\zeta^*a^2-\tfrac{1}{2}\zeta(a^\dagger)^2] \ , \tag{36}$$

and suppose that these states are to be distinguished by ideal homodyne detection. The signal states in (35) have amplitudes squeezed in the X_0 quadrature, so that $\theta=0$ will be assumed. In the absence of noise, the output distribution for input state $|y,r\rangle$ is given by [18,32]

$$\begin{aligned}\hat{p}(x|y,r)&=|\langle x|y,r\rangle|^2\\ &=[2e^{2r}/\pi]^{1/2}\exp[-2(x-y)^2e^{2r}] \ .\end{aligned}$$

Equations (34a) and (34b) then yield the general result

$$\begin{aligned}\hat{p}_\Gamma(x|y,r)=&[\pi(n_\gamma+\tfrac{1}{2}e^{-2r})^{-1/2}\\ &\times\exp[-(x-y)^2/(n_\gamma+\tfrac{1}{2}e^{-2r})]\end{aligned} \tag{37}$$

for the output distribution when Gaussian noise of variance n_γ is present.

Assuming the squeezing parameter r is held fixed, the average energy per signal is given by [18,32]

$$n_s=\sinh^2 r+\int dy\, \xi(y)y^2 \ , \tag{38}$$

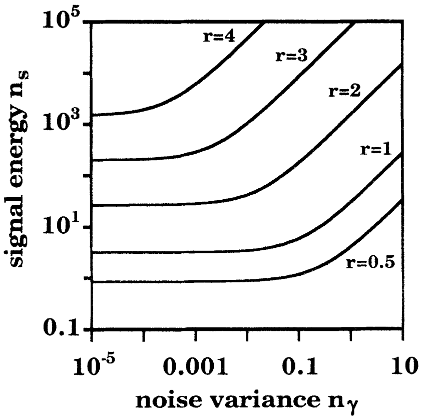

FIG. 1. Contour plot of the optimal squeezing parameter r for the squeezed-state channel of Sec. III C, with $\exp(2r)$ given by the argument of the logarithm in Eq. (40).

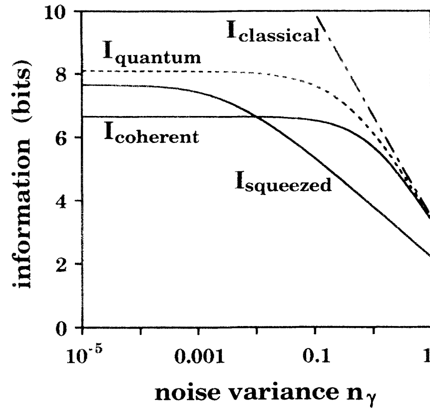

FIG. 2. Channel capacity versus noise variance for the coherent and squeezed-state channels (solid lines); plotted from Eqs. (30) and (40) for an average signal energy $n_s=100$. The crossover point follows from Eq. (41) as $n_\gamma=1/99$. The quantum upper bound (21) and the classical upper bound (23) are also plotted for comparison purposes (dotted and dot-dashed lines respectively).

where $\xi(y)$ denotes the prior probability of transmitting state $|y,r\rangle$. In analogy with Sec. III B, Eqs. (37) and (38) are equivalent to the case of a classical channel with additive Gaussian noise and a quadratic constraint, and the capacity of the channel for fixed r follows as [5]

$$I^{\text{sq}}(n_s,n_\gamma,r)=\tfrac{1}{2}\ln[1+2(n_s-\sinh^2 r)/(n_\gamma+\tfrac{1}{2}e^{-2r})] \;. \quad (39)$$

Finally, optimization over r in (39) yields a "best" channel capacity per symbol of

$$I^{\text{sq}}(n_s,n_\gamma)=\ln\left[\frac{(1+4n_\gamma[2n_s+n_\gamma+1])^{1/2}-1}{2n_\gamma}\right] , \quad (40)$$

where $\exp(2r)$ is given by the argument of the logarithm in (40).

The dependence of the optimal choice of squeezing parameter on n_s and n_γ is indicated in Fig. 1, and it is seen that *zero* squeezing becomes optimal as the noise level increases. The zero noise case ($n_\gamma=0$) has been discussed in [18,26]. From Eqs. (30) and (40) it follows that the squeezed-state channel outperforms the coherent-state channel of Sec. III B whenever the product $n_\gamma(n_s-1)$ is less than unity, i.e.,

$$I^{\text{sq}}(n_s,n_\gamma)\geq I^{\text{coh}}(n_s,n_\gamma) \quad \text{if and only if } n_\gamma(n_s-1)\leq 1 \;. \quad (41)$$

This result is illustrated in Fig. 2 for the choice $n_s=100$ and is discussed further in Sec. III E.

D. Photodetection of number states

The last type of quantum channel to be considered here is based on the particle aspect of light. To be particular then, suppose that the photon-number state $|n\rangle\langle n|$ is transmitted with prior probability ξ_n, and that an ideal measurement of photon number is made at the receiver. If a number-state channel is subject to Gaussian noise of variance n_γ, the mutual information follows from (15a), (20a), and (20b) as

$$I=-\sum_m \bar{\xi}_m \ln\bar{\xi}_m-\sum_n \xi_n H_n \;, \quad (42a)$$

where

$$\bar{\xi}_m=\sum_n R_{mn}^{(0)}(n_\gamma)\xi_n \;, \quad (42b)$$

$$H_n=-\sum_m R_{mn}^{(0)}(n_\gamma)\ln R_{mn}^{(0)}(n_\gamma) \;. \quad (42c)$$

To determine channel capacity, consider the variational quantity

$$J=I-\lambda\left[\sum_n \xi_n-1\right]-\mu\left[\sum_n n\xi_n-n_s\right] , \quad (43)$$

where λ and μ are Lagrange multipliers constraining the normalization of $\{\xi_n\}$ and the average signal energy n_s. Using (18a) and the properties

$$\sum_m R_{mn}^{(0)}(n_\gamma)=1, \quad \sum_n nR_{mn}^{(0)}(n_\gamma)=m+n_\gamma \;, \quad (44)$$

following from (12) and (15a), the extremal equations $\partial J/\partial\xi_n=0$ may be solved for the optimal prior distribution $\{\xi_n\}$, to give

$$\xi_n=\sum_m R_{mn}^{(0)}(-n_\gamma)Z^{-1}\exp\left[-\beta m-\sum_n R_{mn}^{(0)}(-n_\gamma)H_n\right] , \quad (45a)$$

where

$$Z=\sum_m \exp\left[-\beta m-\sum_m R_{mn}^{(0)}(-n_\gamma)H_n\right] . \quad (45b)$$

The parameter β is determined implicitly by the average signal energy via the relation

$$n_s=\sum_n n\xi_n=-\frac{\partial}{\partial\beta}\ln Z-n_\gamma \;, \quad (46)$$

following from (44), (45a), and (45b).

The channel capacity per symbol can now be calculated by substituting Eqs. (45) into (42), yielding the "thermodynamic" expression

$$I^{\text{num}}(n_s,n_\gamma)=\ln Z-\beta\frac{\partial}{\partial\beta}\ln Z\ . \tag{47}$$

For the case of zero noise ($n_\gamma=0$), $R^{(0)}(-n_\gamma)$ reduces to the identity matrix, implying $Z=(1-e^{-\beta})^{-1}$, and leading to the well known result [17,31,33]

$$I^{\text{num}}(n_s,0)=\ln(n_s+1)+n_s\ln(1+1/n_s)\ . \tag{48}$$

This capacity in fact attains the quantum upper bound (45) for the zero-noise case (see [13,18,34] for further discussion), implying that the number-state channel has near-optimal information properties for sufficiently low noise levels.

More generally $n_\gamma>0$, and the channel capacity (47) must be evaluated numerically (see Sec. III E). However, for $n_\gamma \ll 1$ and $n_\gamma n_s \gtrsim (4\pi e)^{-1}$, one has the approximate formula (see Appendix)

$$I^{\text{num}}(n_s,n_\gamma)\approx\tfrac{1}{2}\ln\left[\frac{e^{1+C}}{4\pi}\frac{n_s}{n_\gamma}\right]\ , \tag{49}$$

where $C\approx0.5772157$ denotes Euler's constant. Note that this is approximately one-half of the classical channel capacity (23). The restriction $n_\gamma \ll 1$ is physically relevant since, for example, thermal radiation of temperature $T\sim300$ K and frequency $f\sim10^{14}$ Hz corresponds to a noise variance $n_\gamma\sim10^{-7}$. Approximation (49) is explored further in the following section.

E. Comparisons

A plot of channel capacity versus average signal energy is given in Fig. 3 for the coherent state, squeezed-state, and number-state channels discussed in Secs. III B, III C, and III D, respectively. The noise variance is chosen to be $n_\gamma=10^{-3}$, and the capacity upper bound (21) is also plotted. The figure indicates that the number-state, squeezed-state, and coherent-state channels each become optimal in turn as the average signal energy n_s increases.

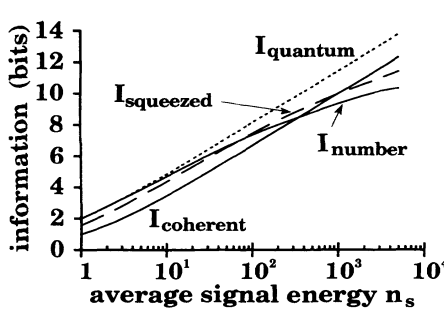

FIG. 3. Channel capacity versus average signal energy for the coherent-state, squeezed-state, and number-state channels; plotted from Eqs. (30), (40), and (47) for the choice $n_\gamma=10^{-3}$. Approximations for the crossover points are given in Eqs. (50a), (50b), and (50c). The dotted line indicates the quantum upper bound (21).

Further, Eqs. (30), (41), and (48) imply that the ordering of optimality remains the same if instead the noise variance n_γ is increased for a fixed value of n_s [though note from (41) that the coherent-state channel never actually achieves optimality if $n_s\le1$].

Approximation (49) for the capacity of the number-state channel may be used to predict the crossover points in Fig. 3. In particular, for $n_\gamma\ll1$ one finds from (30), (40), (41), and (49) that

$$I^{\text{num}}(n_s,n_\gamma)\approx I^{\text{sq}}(n_s,n_\gamma)\quad\text{for } n_\gamma n_s\approx\frac{8\pi e^{1+C}}{(16\pi-e^{1+C})^2}\approx0.051\ , \tag{50a}$$

$$I^{\text{num}}(n_s,n_\gamma)\approx I^{\text{coh}}(n_s,n_\gamma)\quad\text{for } n_\gamma n_s\approx\frac{e^{1+C}}{4\pi}\approx0.385\ , \tag{50b}$$

$$I^{\text{sq}}(n_s,n_\gamma)\approx I^{\text{coh}}(n_s,n_\gamma)\quad\text{for } n_\gamma n_s\approx1\ . \tag{50c}$$

Equations (50) are in good agreement with Fig. 3, and in general indicate that the qualitative features differentiating performance depend upon the *product* of the signal and noise energies, at least for the case $n_\gamma\ll1$.

IV. DISCUSSION

Gaussian noise is seen to provide a generic model for the effects of random linear excitations on single-mode fields (Sec. II A). The various properties noted in Sec. II B are therefore expected to have a wide range of applicability, particularly in regard to determining the robustness of various quantum-optical systems with respect to noise.

One obvious application, motivated by analogy with classical information theory, is to study the effects of Gaussian noise for quantum communication channels. While preliminary results are given in Sec. III, the optimal channels discussed there are rather more theoretical than practical in interest, as the corresponding channel capacities (30), (39), (40), and (47) rely on the availability of an infinite choice of signal states and zero signal attenuation.

It is important to also make noise calculations for channels based on the transmission of a small number of signal states and to model signal losses. Results such as the perturbation expansion (14), the number-state representation (15), and expressions (25), (26), and (34) for the effects of Gaussian noise on heterodyne and homodyne statistics may be of use to such calculations, while the thermal noise model in [16] may be useful for modeling the combined effects of Gaussian noise and attenuation. Note that Helstrom [4] and Yoshitani [8] have examined error rates for channels based on transmission of two coherent states in the presence of noise, Vourdas [35] has numerically calculated error and information rates for channels based on the transmission of two number states, and first-order results for the error rates of general number-state channels degraded by noise are given in [13].

A primary motivation for studying the coherent-state, squeezed-state, and number-state channels in Secs. IV B, IV C, and IV D, respectively, was to determine the relative robustness of various properties of light with respect to noise. In particular, these channels respectively exploit wave, quadrature-amplitude, and particle properties of radiation. Results indicate that it is the *wavelike* coherent-state channel of Sec. IV B that is the most stable when either noise energy or signal energy is increased, while the *particlelike* number-state channel of Sec. IV D is the least stable [see Figs. 2 and 3 and Eqs. (50a), (50b), and (50c)]. This "information" stability of the semiclassical coherent states, in the limits of high noise and high signal energies, is related to a minimum-entropy property of these states in the presence of noise [13,36], and hints at a strong connection between noise and classical decoherence [36,37]. It would be of interest to determine the robustness of channels based on the *phase* properties of light (some results for the zero-noise case are given in [38]).

Finally, it should be remarked that the assumptions used in Sec. II to derive the Gaussian noise model place limits on its physical applicability. For example, the amplitude correlation function for a state ρ subject to Gaussian noise follows from (6), (7), (9), (11), and (19c) as

$$\begin{aligned}\langle a^{\dagger}(0)a(t)\rangle &= \mathrm{tr}[a^{\dagger}e^{-iN\omega t}\Gamma(a)e^{iN\omega t}\rho] \\ &= \mathrm{tr}[a^{\dagger}e^{-iN\omega t}ae^{iN\omega t}\rho] \\ &= e^{-i\omega t}\langle a^{\dagger}(0)a(0)\rangle \ , \end{aligned} \tag{51}$$

and thus the spectral density function, proportional to the Fourier transform of (51) [39], is a δ function peaked at ω. Hence Gaussian displacement noise is inappropriate for modeling line-broadening processes. This limitation is essentially due to the linear nature of the excitations assumed in Sec. II (as is well known, Lorentzian line shapes can be obtained from the Gaussian *phase* noise model (8) [39]).

ACKNOWLEDGMENTS

I am grateful to Ian Fuss for introducing me to Gaussian noise and to Carlton Caves for a copy of Ref. [18] prior to publication. I thank Robyn Hall for financial support.

APPENDIX

Approximation (49) of the text, for the capacity of number-state channels degraded by Gaussian noise, is derived here via simple arguments. More sophisticated analyses based on Eqs. (45a) and (45b) do not appear to give significantly improved results.

First, noting that the optimal prior distribution for the zero-noise case follows from (45) and (47) as the thermal distribution,

$$\xi_n = n_s^n/(n_s+1)^{n+1} \ , \tag{A1}$$

it will be assumed that this distribution remains approximately optimal for $n_\gamma \ll 1$. Hence, using (14), (17), and (42b) of the text,

$$\bar{\xi}_m = (n_s+n_\gamma)^m/(n_s+n_\gamma+1)^{m+1} \ . \tag{A2}$$

For $n_\gamma \ll 1 \ll n_s$, the channel capacity then follows from (A2) and (20a) as

$$\begin{aligned} I &\approx \ln[n_s+n_\gamma+1]+(n_s+n_\gamma)\ln[1+(n_s+n_\gamma)^{-1}] \\ &\quad -\sum_n \xi_n H_n \\ &\approx \ln n_s e - \sum_n \xi_n H_n \ . \end{aligned} \tag{A3}$$

To estimate H_n in (A3), it will be assumed that the photon-number distribution of $\Gamma(|n\rangle\langle n|)$ is approximately Gaussian for $n_\gamma \ll 1 \ll n$, i.e.,

$$R^{(0)}_{m,n}(n_\gamma) \approx \frac{1}{\sqrt{2\pi}\sigma_n} \exp[-(m-\mu_n)^2/(2\sigma_n^2)] \ . \tag{A4}$$

The mean value μ_n and variance σ_n^2 are determined via (11) and (12) as

$$\mu_n = n+n_\gamma \approx n, \quad \sigma_n^2 = n_\gamma(2n+n_\gamma+1) \approx 2n_\gamma n \ . \tag{A5}$$

Note that Eq. (16) and the asymptotic expansion of Jacobi polynomials (theorem 8.21.7 of [40]) imply

$$R^{(0)}_{n,n}(n_\gamma) = (4\pi n n_\gamma)^{-1/2} + 0(n^{-3/2}) \ ,$$

in agreement with (A4) and (A5), while the intensity distribution for a *classical* signal of intensity J degraded by Gaussian noise follows from Eq. (2.4.11) of [41] as

$$P(I|J) = (2n_\gamma)^{-1}\exp[-(I+J)/n_\gamma]I_0(2\sqrt{IJ}/n_\gamma) \ ,$$

which for n_γ, $|I-J| \ll 1$ reduces to

$$P(I|J) \approx (4\pi n_\gamma J)^{-1/2}\exp[-(I-J)^2/(4n_\gamma J)] \ ,$$

in direct analogy with (A4) and (A5).

From (A4), (A5), and (42c), one may approximate the entropy H_n by the entropy of a (continuous) Gaussian distribution of variance σ_n^2, i.e.,

$$H_n \approx \tfrac{1}{2}\ln 4\pi e n_\gamma n \ . \tag{A6}$$

This approximation is checked numerically in Fig. 4 for the case $n_\gamma = 10^{-3}$. It is sensible only for $n_\gamma n \geq (4\pi e)^{-1}$

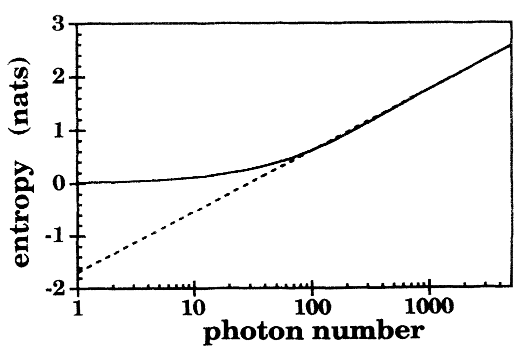

FIG. 4. Entropy of the nth photon-number state when degraded by Gaussian noise, plotted from Eq. (42c) for the choice $n_\gamma = 10^{-3}$ (solid line) and the corresponding approximation (A6) of the Appendix (dotted line). The ordinate units correspond to the choice of the natural logarithm base e in Eqs. (42c) and (A6) (see Sec. III A).

to ensure a positive entropy, and hence this inequality will be assumed to hold on average in what follows, i.e., it will be assumed that $n_\gamma n_s \geq (4\pi e)^{-1}$ in addition to $n_\gamma \ll 1 \ll n_s$. It may be checked via (14) that $H_0 \approx 0$ for $n_\gamma \ll 1$, and hence from (A1) and (A6) it follows that

$$\sum_n \xi_n H_n \approx \tfrac{1}{2}\ln 4\pi e n_\gamma + \tfrac{1}{2}(n_s+1)^{-1} \sum_{n>0} \left[\frac{n_s}{n_s+1}\right]^n \ln n$$
$$\approx \tfrac{1}{2}\ln 4\pi e n_\gamma + (2n_s)^{-1}\int_1^\infty dx\, \exp(-x/n_s)\ln x$$
$$= \tfrac{1}{2}\ln 4\pi e n_\gamma + \tfrac{1}{2}E_1(n_s^{-1}) , \qquad (A7)$$

where E_1 denotes the first-order exponential integral [25], and $n_s \gg 1$ has been assumed. But for $x \ll 1$, one has $E_1(x) \approx -C - \ln x$ [Eq. (5.1.11) of [25]], where $C = 0.577\,215\,66\ldots$ denotes Euler's constant. Hence combining (A3) and (A7), one has the final approximation

$$I \approx \ln n_s e - \tfrac{1}{2}\ln 4\pi e n_\gamma - \tfrac{1}{2}(-C + \ln n_s)$$
$$= \tfrac{1}{2}\ln\left[\frac{n_s}{n_\gamma}\frac{e^{1+C}}{4\pi}\right] \qquad (A8)$$

for the channel capacity per symbol, as given in Eq. (49) of the text.

[1] M. Born and E. Wolf, *Principles of Optics* (Pergamon, London, 1959), Chap. 10.
[2] J. W. Goodman, *Statistical Optics* (Wiley, New York, 1985), Secs. 2.6 and 2.9.
[3] H. L. Van Trees, *Detection, Estimation, and Modulation Theory Part I* (Wiley, New York, 1968), Secs. 1.1 and 3.3.3.
[4] C. W. Helstrom, *Quantum Detection and Estimation Theory* (Academic, New York, 1976).
[5] R. G. Gallagher, *Information Theory and Reliable Communication* (Wiley, New York, 1968), Secs. 4.2, 7.4, and 7.5.
[6] R. J. Glauber, Phys. Rev. **131**, 2766 (1963).
[7] G. Lachs, Phys. Rev. **138**, B1012 (1965).
[8] R. Yoshitani, J. Stat. Phys. **2**, 347 (1970).
[9] A. Vourdas, Phys. Rev. A **34**, 3466 (1986).
[10] H. Fearn and M. J. Collett, J. Mod. Opt. **35**, 553 (1988).
[11] R. Loudon and T. J. Shepherd, Opt. Acta **31**, 1243 (1984).
[12] A. Vourdas, Phys. Rev. **37**, 3890 (1988).
[13] M. J. W. Hall and M. J. O'Rourke, Quantum Opt. **5**, 161 (1993).
[14] E. Merzbacher, *Quantum Mechanics,* 2nd ed. (Wiley, New York, 1970), pp. 287 and 288.
[15] C. T. Lee, in *Workshop on Squeezed States and Uncertainty Relations (NASA Conference Publication 3135),* edited by D. Han *et al.* (NASA, Washington DC, 1991), pp. 365–367.
[16] C. W. Helstrom, J. Math. Phys. **20**, 2063 (1979).
[17] D. S. Lebedev and L. B. Levitin, Inf. Control **9**, 1 (1966); J. D. Bekenstein and M. Schiffer, Int. J. Mod. Phys. C **1**, 355 (1990).
[18] C. M. Caves and P. D. Drummond, Rev. Mod. Phys. **66**, 481 (1994).
[19] W. H. Louisell, *Quantum Statistical Properties of Radiation* (Wiley, New York, 1973), Secs. 3.1 and 3.4.
[20] M. Hillery, R. F. O'Connell, M. O. Scully, and E. P. Wigner, Phys. Rep. **106**, 121 (1984).
[21] S. Carusotto, Phys. Rev. A **11**, 1629 (1975).
[22] E. B. Rockower, N. B. Abraham, and S. R. Smith, Phys. Rev. A **17**, 1100 (1978).
[23] S. Friberg and L. Mandel, Opt. Commun. **46**, 141 (1983).
[24] I. G. Fuss and M. J. W. Hall, in *Proceedings of the 1990 IASTED International Symposium on Signal Processing and its Applications Volume 2,* edited by B. Boashash and P. Boles (Uniquest Ltd., Brisbane, 1990), p. 714.
[25] *Handbook of Mathematical Functions,* edited by M. Abramowitz and I. A. Stegun (Dover, New York, 1965), Chaps. 5 and 22.
[26] Y. Yamamoto and H. A. Haus, Rev. Mod. Phys. **58**, 1001 (1986).
[27] E. B. Davies, *Quantum Theory of Open Systems* (Academic, New York, 1976), Sec. 3.1.
[28] H. P. Yuen and J. H. Shapiro, IEEE Trans. Inf. Theory **IT-26**, 78 (1980).
[29] J. H. Shapiro and S. S. Wagner, IEEE J. Quantum Electron. **QE-20**, 803 (1984).
[30] M. J. W. Hall and I. G. Fuss, Quantum Opt. **3**, 147 (1991).
[31] J. P. Gordon, Proc. IRE **50**, 1898 (1962).
[32] R. Loudon and P. L. Knight, J. Mod. Opt. **34**, 709 (1987).
[33] T. E. Stern, IRE Trans. Inf. Theory **IT-6**, 435 (1960).
[34] H. P. Yuen and M. Ozawa, Phys. Rev. Lett. **70**, 363 (1993).
[35] A. Vourdas, IEEE Trans. Inf. Theory **IT-36**, 208 (1990).
[36] W. H. Zurek, S. Habib, and J. P. Paz, Phys. Rev. Lett. **70**, 1187 (1993).
[37] M. J. W. Hall, Phys. Rev. A **49**, 42 (1994).
[38] M. J. W. Hall, J. Mod. Opt. **40**, 809 (1993).
[39] A. Yariv, *Optical Electronics,* 4th ed. (Holt, Rinehart and Winston, Orlando, 1991), Chap. 10.
[40] G. Szegö, *Orthogonal Polynomials,* American Mathematical Society Colloquium Publications Vol. 23 (American Mathematical Society, New York, 1939), Chap. 8.
[41] R. M. Gagliardi and S. Karp, *Optical Communications* (Wiley, New York, 1976), Sec. 2.4.